LASER SPECTROSCOPY IN MOLECULAR BEAMS: AN AUTOMATED SYSTEM FOR OBTAINING HIGH RESOLUTION SPECTRA OF LARGE MOLECULES

B. W. Keelan, J. A. Syage, J. F. Shepanski, and A. H. Zewail*

Arthur Amos Noyes Laboratory of Chemical Physics**

California Institute of Technology

Pasadena, California 91125 USA

Abstract

A nanosecond laser pulsed molecular beam apparatus designed to obtain excitation and dispersed fluorescence spectra of cold molecules is described in detail. Typical spectra are presented to demonstrate the capabilities of the system.

I. Introduction

As our work on picosecond dynamics of large molecules has been reviewed in detail elsewhere,[1] in this paper we shall describe our nanosecond laser pulsed molecular beam apparatus which complements the picosecond apparatus.

In order to study energy redistribution on the ps time scale, it is first necessary to understand the vibronic structure of the molecule in question. Two extremely important methods for probing such structure are excitation and dispersed fluorescence spectroscopy.

In an excitation spectrum, the fluorescence is collected as a function of excitation energy. In a dispersed fluorescence experiment, the excitation energy is fixed at a value where the molecule is known to absorb, and the fluorescence is wavelength-resolved. The excitation and dispersed fluorescence experiments probe the vibronic structures of the excited and ground states respectively. These spectra may be greatly simplified if the molecules are cooled, which reduces sequence congestion and hot bands (vibrational cooling) and narrows linewidths (rotational cooling). A supersonic molecular beam can cool isolated molecules below their condensation temperature, allowing them to be studied in the absence of complicated intermolecular perturbations.

The density of large molecules in a molecular beam is generally very low, hence a powerful tunable ultraviolet (UV) source is required, as well as a sensitive detection system. Herein we describe such an apparatus and present spectra demonstrating its capabilities and performance.

II. The Molecular Beam

A. Hardware

There are a number of advantages of pulsed molecular beams over continuous molecular beams, most of which are related to the reduced pumping requirements. Higher backing pressures and larger apertures may be used in pulsed systems, which improves cooling and results in higher densities of the sample molecules. Sample consumption is minimal in pulsed systems. The gated detection used in pulsed systems reduces the noise due to external light dramatically.

Our molecular beam is one of the most compact in use today. The 4" diameter chamber is pumped down to below 100 μtorr (valve closed) by a 4" diffusion pump. The chamber is equipped with two pairs of mutually orthogonal opposing portals which are in turn orthogonal to the beam axis. One pair is used for the detection system and viewing of the nozzle arrangement. The other pair has Brewster angle quartz windows to allow maximum transmission of the UV laser beam.

In Fig. 1 a simplified diagram of the pulsed valve assembly is presented. Initially the spring seals the pin against the aperture and the magnetic core is in contact with the front o-ring. When the solenoid is actuated, the magnetic core is accelerated backward. Before contacting the lip of the pin, the core has attained nearly final velocity, hence when contact is made, the aperture is opened with a very short rise time. After current has ceased to flow through the solenoid, the core contacts the back o-ring, which reverses the direction of its motion. The assembly is returned to its initial configuration by the spring, resealing the aperture. The aperture seat is made out of aluminum, the pin out of a hard plastic, Vespel.

The diameter of the pinhole may be reduced from the 750 μm bore size by inserting apertures designed for electron microscopy. The pulsed valve is capable of operating at repetition rates in excess of 50 Hz, however, we are limited to 20 Hz by the laser system. Gas pulse widths are typically 300 μs although pulses widths below 200 μs have been produced. Under normal running conditions (10 Hz, 50 psi Ne, and 300 μm aperture), the ambient pressure in the chamber is $\approx$ 200 μtorr. The accessibility of the sample holder allows rapid sample refills and convenient cleaning.

The valve assembly may be heated as high as 475 K. The temperature is monitored by two chromel-alumel thermocouples, one located at the sample holder and one away from the sample to detect any thermal gradients (in practice the readings differ by only a few K). Two 40 W cartridge heaters are controlled by a digital monitor which utilizes the thermocouple readings in a feedback loop. The set point temperature is stable to better than a K indefinitely.

The entire valve assembly is mounted on a vacuum-sealed x-y-z translatable mount to allow adjustment of the nozzle to laser distance and optimization of beam alignment for excitation and detection.

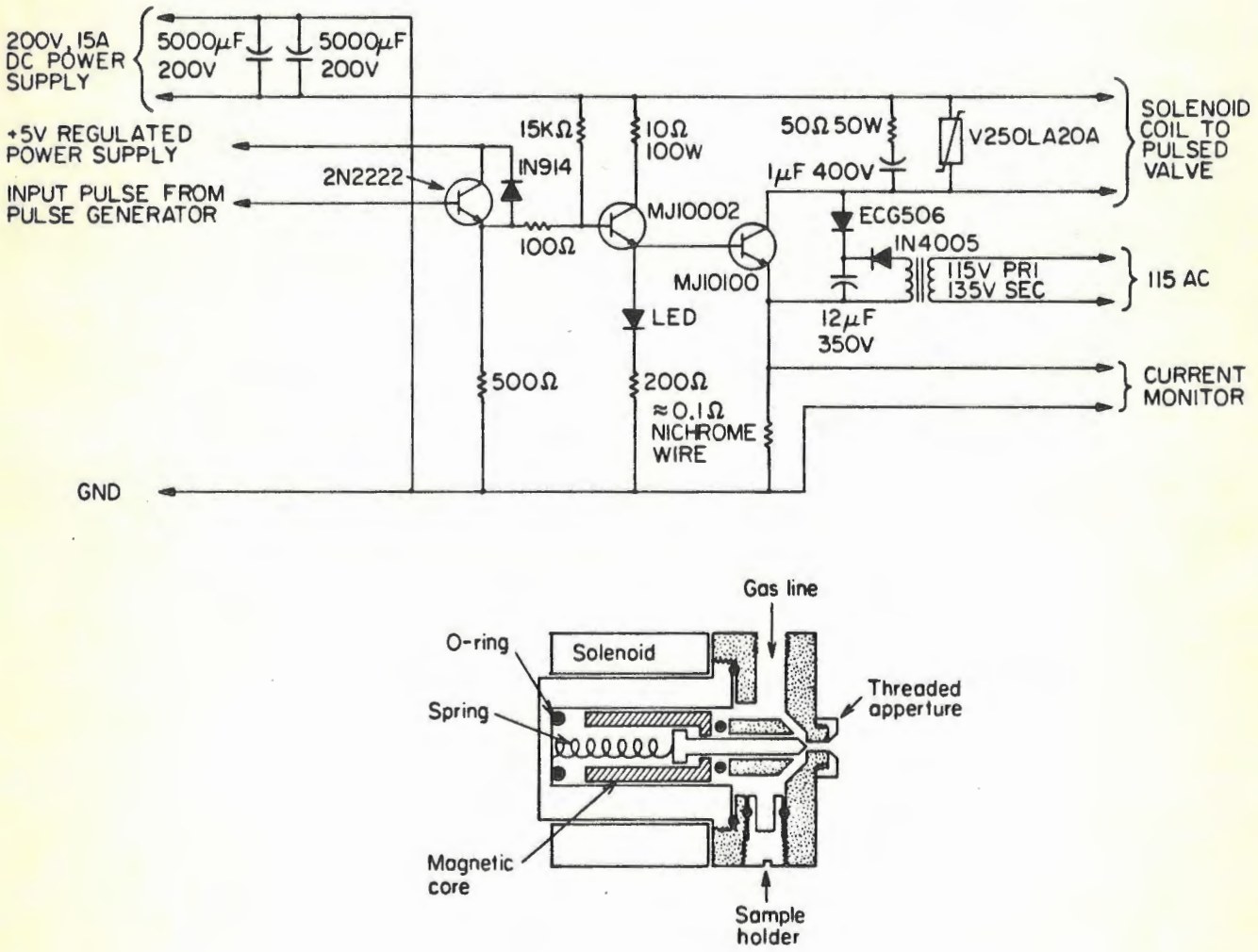

Fig. 1: Analog switching circuitry and pulsed valve schematic. A capacitor bank is charged by a DC power supply and then discharged through a series of transistors upon triggering. The amplified pulse activates the valve solenoid, accelerating the magnetic core, and in turn lifting the pin. The core motion is reversed by the back o-ring, and the pin is restored to its initial position by the spring. The resulting gas pulse is typically 300 μs long. For simplicity, the thermocouples and cartridge heaters are not shown.

B. Electronics

The electronics controlling the actuation of the solenoid and the triggering of the laser were built in our laboratory. The control box is essentially a dual pulse generator. The two pulsed outputs may be adjusted independently for pulse duration and pulse delay (both 5μs - 5 ms) from a reference trigger, either internal or external. The repetition rate may be set from 0.1 - 50 Hz. These quantities, as well as total number of pulses, may all be displayed on a digital readout with a variable sampling time.

One of the pulsed outputs is amplified from 5 V (TTL) to 15 V (CMOS) and used to trigger the laser system. The other pulsed output is passed through an optoisolator and triggers the pulsed amplifier. A diagram of the pulsed amplifier circuitry is given in Fig. 1. A DC power supply is used to charge large capacitors which are then rapidly discharged by a series of transistors. The high peak power pulse (100 V, ≈ 100 A) actuates the low inductance solenoid in the valve. The MJ10002 and MJ10100 high power switching transistors provide the major current amplification. The 2N2222 boosts the current of the optoisolated TTL pulse to an acceptable level for the MJ10002.

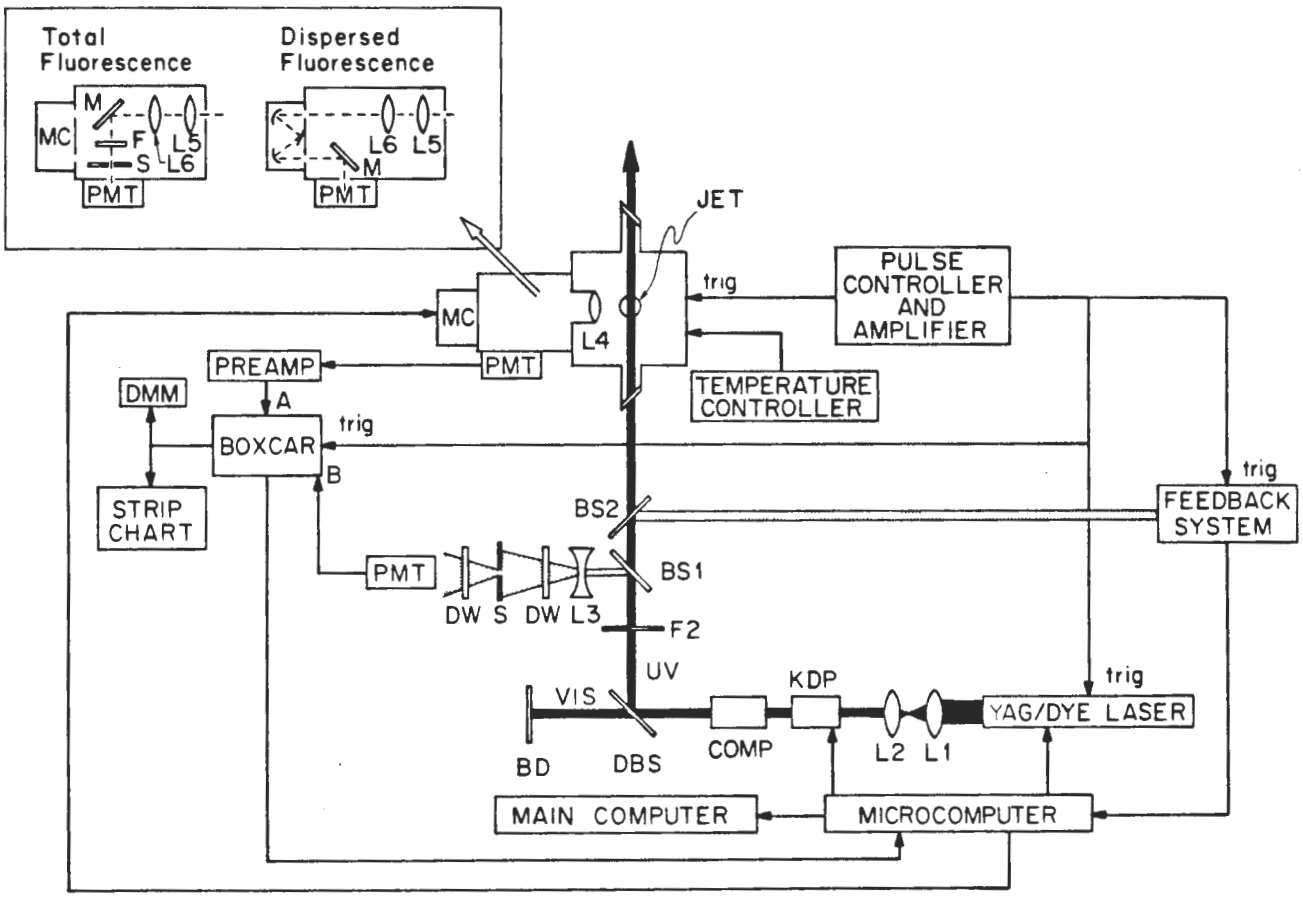

Fig. 2: Schematic of the nanosecond laser pulsed molecular beam apparatus. The configuration of the detection optics is illustrated for recording both excitation and dispersed fluorescence spectra. Abbreviations: L = lens; F = filter; M = mirror; S = slit; BS = beam splitter; DBS = dichroic beam splitter; DW = diffusing window; MC = monochromator; COMP = compensator; DMM = digital multimeter; BD = beam dump; PMT = photomultiplier tube.

High speed circuits protect against the backlash induced by the magnetic core returning to its initial position. A fast diode (ECG506) and a 135 VAC source, rectified with a capacitor and 1N4005 diode, generates a 200 VDC clamp on the reverse voltage. If the reverse voltage does exceed this value, the diode becomes reverse biased, passes current, and thereby prevents excessive voltage from being applied to the MJ10100. Additional protection is offerred by the V250LA20A varistor. The MJ10002 and MJ10100 power transistors and the 50 Ω, 50 W resistor assembly (two parallel 100 Ω, 25 W elements) are mounted on heat sinks. A fan and vent provide circulation of air over all the components.

III. Generation of Tunable Radiation

A. Lasers

Tunability is most readily achieved in the visible region, using dye lasers. Our pulsed dye laser (PDL) is pumped by a frequency-doubled YAG laser at 532 nm, producing 540 - 800 nm radiation. This is frequency-doubled to generate 270 - 400 nm UV. At 10 Hz, the PDL output can be as high as 25 mJ/pulse (peak power 5 MW).

Frequency-doubling of the YAG is effected by passing the laser beam through a KDP crystal cut to the proper phase-matching angle. KDP is preferable to $LiIO_3$ due to its much higher damage threshold. The crystal mount may be rotated about three mutually orthogonal axes to enable fine tuning of the orientation. The phase-matching angle is very sensitive to temperature changes, which can produce substantial long term power fluctuations. It is necessary to separate the 75 % of the 1064 nm which is not frequency-doubled from the 532 nm before dye-pumping. This is effected by a series of two high damage threshold 45° dichroic mirrors which transmit 1064 nm but reflect 532 nm. These are mounted in x-y mounts to facilitate alignment of the beam into the PDL. The ≈ 2 W of 1064 nm passing through the first dichroic is dumped into a 10 cm water cell encased in a protective box just outside the PDL.

B. Frequency-doubling of PDL Output

It will be helpful in this and the following subsections to refer to Fig. 2. Parenthetical abbreviations pertain to that figure.

The PDL output is steered by two antireflection-coated 90° turning prisms. The beam diameter is then reduced by a factor of ≈ 3 by a simple two lens telescope (L1, L2). This increases the light intensity by nearly an order of magnitude, with a corresponding increase in frequency-doubling efficiency. The beam divergence is increased by the reduction factor, preventing the use of even higher reduction factors.

The light is then doubled by an appropriately-cut KDP crystal with up to 5 % efficiency. The effective phase-matching angle of the crystal can be varied by tilting the crystal. A fixed angle will typically frequency-double wavelengths spanning only a few nm in the UV but tilting the crystal can result in a tuning range of ≈ 100 nm. This, however, introduces a variable displacement in the beam path which would necessitate frequent realignment of the optics if not corrected. To eliminate this displacement we have constructed a compensator, utilizing a liquid cell (COMP) with the same index of refraction and path length as the KDP crystal assembly. The crystal and cell are mounted on counter-rotating wheels which may be disengaged for initial synchronization. The liquid cell has quartz windows and is filled with CCl_4. We have found the liquid cell superior to a solid quartz cube compensating element both in terms of UV transmission and beam quality.

The beam is then directed to one of two high damage threshold 45° dichroic mirrors (DBS) which transmit PDL output but reflect UV. Transmitted PDL may be beam-dumped, used for triggering, etc. The two dichroics, which cover different wavelength regions, are attached to a translating stage, and can be interchanged without affecting the alignment of the system. The dichroics are mounted in x-y mounts, facilitating steering of the beam into the vacuum chamber.

The entire optics assembly described above is covered by a removable 2.5 optical density plexiglas box to reduce scattered light. When the laser is operating, it is possible to distinguish each optical component but no intense light escapes. As plexiglas with 2.5 optical density is available only by special order in bulk, the plexiglas for this application was fabricated by laminating three 1/8 " thick sheets of 12 % transmitting gray with (1,2)-dichloroethane. An entrance port was drilled out for PDL input; because of its location, escape of scattered light from this port is minimal. The exit port is a removable UV-transmitting visible-absorbing filter (F2) which eliminates the small amount of PDL output reflected by the UV dichroic mirror.

C. Monitoring of Ultraviolet Radiation

The UV beam propagates from the laser table to a second steel table and passes through two angled quartz windows acting as 10 % beamsplitters (BS1, BS2). One beamsplitter directs light to a 1P28 photomultiplier tube (PMT), which is used to monitor the UV intensity. The output of the power meter is used by the boxcar integrator to normalize the fluorescence signal. This eliminates two potential sources of error in the signal: shot-to-shot variation in the laser power, and variation of dye efficiency with wavelength in an excitation scan. Before reaching the PMT, the UV beam is passed through a diverging lens (L3), a diffusing window (DW), a slit (S), and a second diffusing window to avoid saturation and produce uniform light intensity across the active surface.

The other beamsplitter directs light onto an x-y adjustable aluminum-coated mirror which is used to accurately align the beam between two matched photodiodes, the active surfaces of which are ≈ 3 mm apart. The beam is slightly dispersed using a doubly concave lens so that if the UV beam angle changes slightly, one photodiode will receive more UV than the other. This serves as the basis for a feedback system, described in Sec. IV A, which continuously adjusts the KDP crystal angle as the PDL wavelength is scanned.

The UV which passes through both beamsplitters is reflected upward by an antireflection-coated 90° turning prism. The beam, properly polarized, encounters a Brewster angle quartz window, passes through the molecular beam chamber, encounters a complementary Brewster angle quartz window, exits from the chamber, and is finally terminated on a fluorescent card to allow visual monitoring of the UV intensity and beam quality. In the vacuum chamber the laser beam intersects the molecular beam, excites the molecules under study, and causes them to fluoresce. Detection of this fluorescent signal is discussed in Sec. V.

IV. Computer Control

A. Stepping Motors

A microcomputer is used to control two stepping motors which scan the wavelength on the dye laser or monochromator and adjust the angle of the PDL frequency-doubling KDP crystal. Primitive commands sent from the keyboard of the host computer are used to program two CY500 stepping motor controllers. These devices are specialized peripheral control chips that generate four square wave signals, the frequencies and relative phases of which determine the stepping motor rate and direction. The CY500 output must be amplified prior to driving the stepping motor. In addition to host computer programming, the CY500 accepts external control signals which are used to trigger steps and change motor direction. This feature is used by the frequency-doubling feedback circuit, described below, to continuously adjust the angle of the KDP crystal.

A stepping motor step corresponds to an increment of 0.005 nm on the monochromator or PDL (at grating order 5). The motor used to turn the KDP crystal is geared down so that one motor step changes the crystal's orientation by 0.03°, allowing sufficiently fine adjustment of the angle to achieve high frequency-doubling efficiency.

B. Frequency-doubling Feedback System

The process of frequency doubling requires a condition of index matching of fundamental and second harmonic waves in a birefringent crystal. For a given wavelength this occurs when the fundamental ray is incident at a specific angle, termed the phase-matching angle, from the relevant crystal axis.[2] At the phase-matching angle, the harmonic ray propagates on the same axis as the fundamental. Small deviations from the phase-matching angle (a few tenths of a degree) produce a marked decrease in frequency-doubling efficiency. This is accompanied by an angular divergence of the harmonic ray from the fundamental axis.

As the PDL wavelength is scanned, the UV ray displacement (several mm per meter of path length) is used to activate a feedback circuit, which corrects the angle of the crystal. The sensitivity of the circuit is sufficient to prevent any significant decrease in UV intensity at normal laser scan rates. This circuit allows continuous scanning of the entire wavelength range of a PDL dye without adjustment of any optics.

A block diagram of the feedback circuit is presented in Fig. 3. During initial system adjustment, the UV beam is centered between two matched photodiodes so that they generate equal currents (the diameter of the UV beam is slightly greater than the distance between photodiodes). Any shift in the UV beam position produces a difference in photocurrents, which is used to activate the feedback loop.

Photocurrents generated by a laser pulse are converted to voltages and held by peak detector circuits (see Fig. 3). These circuits, like others in the feedback system, are described in Ref. 3. The two peak detectors are reset before each laser pulse so that they sample shot-to-shot changes in the UV beam position. The output voltage of each detector is sent to three circuits designated as cw/ccw, |diff|, and sum in Fig. 3. The first of these is a comparator that determines which photodiode produces the largest current. This is used to determine whether the stepping motor needs to turn clockwise or counterclockwise in order to correct the crystal angle. The latter two circuits take the sum, V_s , and absolute value of the difference, V_d , between the two peak detector voltages, respectively.

V_s and V_d are used in a rate selecting circuit to determine how rapidly the stepping motor should move. V_s is dropped in steps by a series of resistors. Each divided voltage is compared to V_d . If $V_d < 0.15\ V_s$ the motor is stationary as this indicates nearly perfect adjustment of the crystal. If $0.15\ V_s < V_d < 0.40\ V_s$ or $0.40\ V_s < V_d < 0.70\ V_s$, the motor adjusts the crystal angle at a stepping rate of 10 or 33 Hz, respectively. We have found that when UV intensity is low, shot-to-shot fluctuations in the beam introduce spatial inhomogeneities that can disrupt the tracking of the feedback system. For this reason the rate selecting circuit disables the motor when $V_d > 0.70\ V_s$.

The output of the rate selector is sent to a latch that prevents the motor from stepping during the reset sequence, as circuit noise during this interval was found to produce spurious stepping. The timing of the reset sequence is illustrated at the bottom of Fig. 3. A pulse synchronized with the laser triggers a delay timer. At the end of its period the delay circuit activates two other timed pulses, designated as reset and hold. The first clears the peak detectors and prepares them to sample the next laser pulse. The second activates the latch and prevents stepping motor movement. Between the trailing edges of the reset and hold pulses there is a "timing window" during which the next laser pulse occurs. The position of the timing window is adjusted to the laser frequency using a potentiometer in the delay timer circuit. In rapidly-pulsed or continuous laser systems, the two peak detectors could be replaced by time-averaging circuits and the timing circuits eliminated.

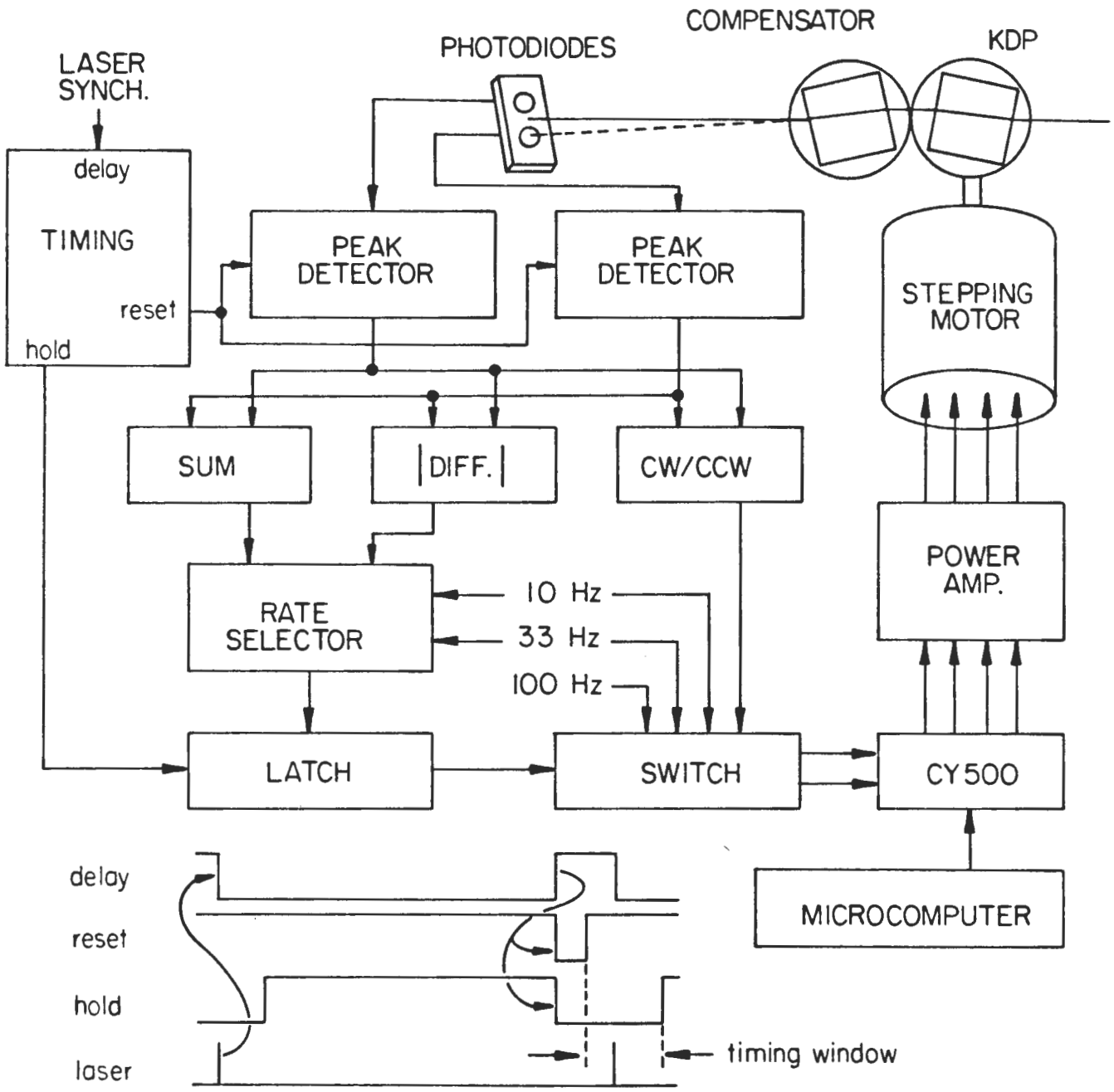

Fig. 3: Frequency-doubling feedback circuitry. During a laser pulse, the photocurrents generated by two matched photodiodes are monitored by two peak detectors. The fractional difference (absolute difference divided by sum) of the peak values is used to determine the stepping rate, while the relative sizes of the peak values are used to determine the stepping direction (cw or ccw). The peak detectors are reset just prior to the next laser pulse. The stepping motor is disabled during the resetting of the peak detectors and the laser pulse to avoid spurious stepping instructions resulting from noise.

Rate and direction information are conveyed to a CY500 stepping motor control chip through a switch. The switch also provides the option of manually adjusting the crystal angle at stepping rates of 10, 33 and 100 Hz. The CY500 is programmed initially by the microcomputer to receive the rate and direction signals from the feedback circuit and step the crystal motor appropriately.

V. Detection and Signal Processing

The lens properties and arrangement described below were optimized using a ray-tracing program written in our laboratory. A useful discussion of the use of field lenses is given in Ref. 4. It will be useful in this section to refer to Fig. 2. Parenthetical abbreviations pertain to that figure.

The fluorescence is collected by an f/1 lens (L4) mounted in the chamber and imaged into an optics housing configured to collect either total or dispersed fluorescence. In both cases, two translatable lenses (L5, L6) allow proper matching of the effective f/ number of the combined three lens system to the monochromator and PMT. The lens system allows variation of the imaged f/ number without changing the image plane, which is coincident with the monochromator entrance slit or the PMT surface, depending on the housing configuration. L5 is a field lens which contains light collected by L4 which would otherwise be lost by divergence in a two lens system. L6 acts as an aperture or "stop" in the excitation region of the jet so that light originating outside of a 5 - 10 mm diameter collection area is not detected. This strongly discriminates against scattered laser light.

For excitation spectra, the imaged light is reflected by a mirror (M) through a choice of filters (F) and an adjustable slit (S) before impinging on the PMT. The slit further reduces the fluorescence collection zone and is used only when the level of scattered light becomes problematical. For recording dispersed fluorescence spectra, the slit and filters are removed and the mirror relocated as shown in the figure. The f/8 half-meter monochromator has a dispersion of 1.6 nm/mm.

The output of the EMI 6256B PMT is fed into the boxcar integrator A channel (a preamp is required for dispersed fluorescence spectra). As stated earlier, the output of a PMT, monitoring laser pulse intensity, is fed into the boxcar B channel. The fluorescence signal is then normalized by using the A/B ratio mode of the gated integrator. An oscilloscope is used to monitor the A and B boxcar inputs, and a digital multimeter (DMM) and strip chart recorder the integrated A/B output. Special care was taken to insure that the PMT outputs were linear with incident photon flux and that the molecular transitions were not saturated by excessive laser power.

The A/B output voltage of the boxcar is fed into a variable gain circuit and then into a voltage-to-frequency converter. A counting circuit digitizes the frequency output. The count is read by the microcomputer and reset each time the PDL or monochromator steps. The digitized voltage is sent to the main computer where the scan is stored on floppy disk and may later be plotted or analyzed for peak positions and intensities.

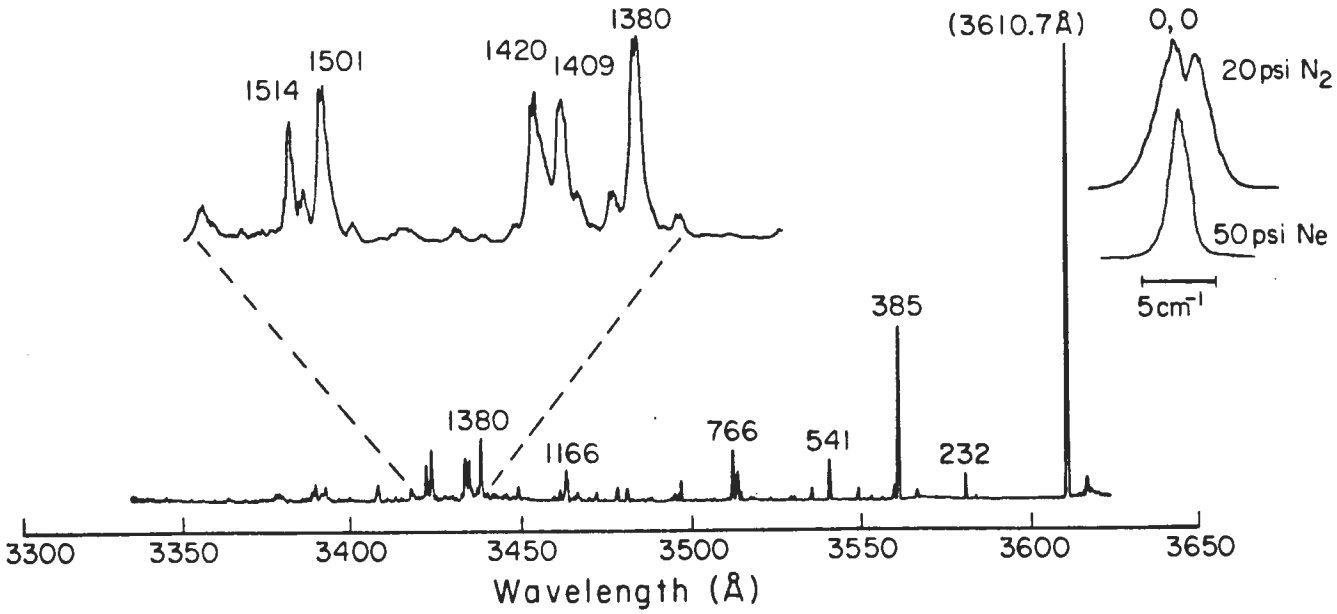

Fig. 4: Representative excitation spectrum of anthracene from Ref. 5. Sample temperature: 405 K; carrier gas: 50 psi N_2. The rotational bandshape of the 0-0 is illustrated under two different cooling conditions. The numbers above bands are the energies relative to the 0-0 in wavenumbers.

VI. Representative Spectra

Typical excitation and dispersed fluorescence spectra obtained with our apparatus are shown in Figs. 4 and 5 respectively.[5] The signal to noise ratio in our experiments is usually one hundred (dispersed fluorescence) to several hundred (excitation). Vibrational cooling is sufficiently complete that less than 1 % of the molecules are in $v > 0$ states, so hot bands are effectively eliminated. Despite the large size of the molecules studied, bandwidths (FWHM) as narrow as 1 cm^{-1} have been observed in excitation scans, indicating effective rotational cooling.[6]

It should be noted that the sytem is somewhat more versatile than has been indicated in this paper. The two-photon excitation spectroscopy of diphenylbutadiene has been investigated by removing the UV-generating optics.[7] By scanning the boxcar gates, time-resolved fluorescence spectra have been obtained.[5] Finally, addition of a differentially-pumped electron-multiplier to the vacuum chamber has allowed ion detection in pump-probe experiments.[8] In total, the performance of the system has proved quite satisfactory with respect to ease of operation, versatility, and reproducibility of spectra.

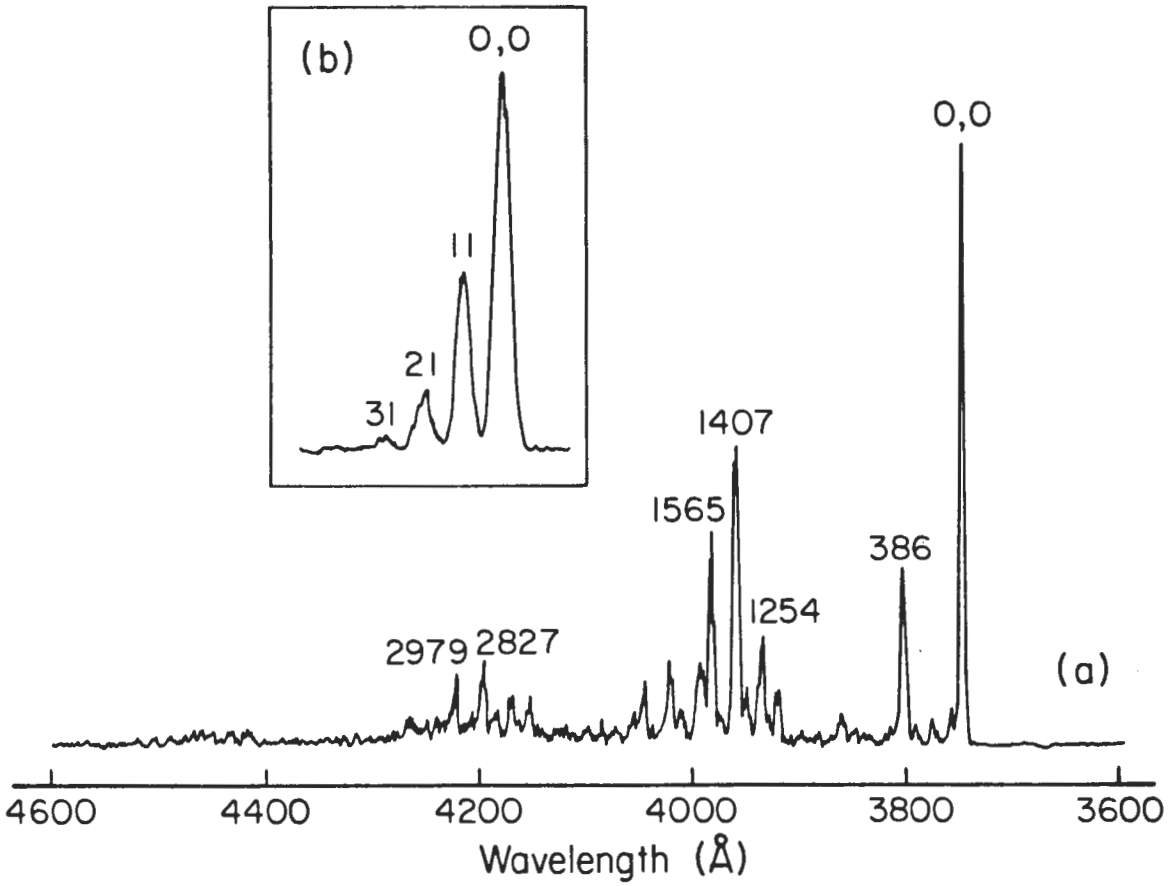

Fig. 5: Dispersed fluorescence spectrum following 0-0 excitation of 9-(3-(para-(N,N-dimethylaniline))propyl)anthracene from Ref. 5. Sample temperature: 435 K; carrier gas: 50 psi Ne. (a) Survey scan. Monochromator resolution: 0.2 nm. (b) High resolution scan of the 0-0 region. Monochromator resolution: 0.05 nm. The numbers above bands are the energies relative to the 0-0 in wavenumbers.

Acknowledgments

This work was supported by National Science Foundation grants CHE-8211356 and DMR-8105034.

References

*Camille and Henry Dreyfus Foundation Teacher-Scholar

**Contribution No. 6983

1. For recent reviews, see: [a] A. H. Zewail, *Faraday Discuss. Chem. Soc.* 75, 315 (1983); [b] P. M. Felker and A. H. Zewail, submitted to *Proceedings of the 1983 NATO Advanced Research Workshop.*

2. A. Yariv, *Quantum Electronics* (New York: Wiley) 1976, Ch. 16.

3. P. Horowitz and W. Hill, *The Art of Electronics* (Cambridge: Cambridge University Press) 1980, Ch. 3.

4. M. V. Klein, *Optics* (New York: Wiley) 1970, Ch. 3, pp. 111 - 116.

5. J. A. Syage, P. M. Felker, and A. H. Zewail, submitted to *J. Chem. Phys.*

6. J. A. Syage, F. Al Adel, and A. H. Zewail, *Chem. Phys. Letts.*, 103, 15 (1983).

7. J. F. Shepanski, B. W. Keelan, and A. H. Zewail, *Chem. Phys. Letts.* 103, 9 (1983).

8. [a] J. W. Perry, N. F. Scherer, and A. H. Zewail, *Chem. Phys. Letts.* 103, 1 (1983); [b] N. F. Scherer, J. F. Shepanski, and A. H. Zewail, to be published.